HYSTERETIC FIELDS IN A TOROIDAL REACTOR

Y.SAITO, S. HAYANO, T. YAMAMURA and H. SAOTOME

Abstract - A modeling of hysteretic fields had been previously proposed for calculating three-dimensional magnetic fields in a toroidal reactor [1]. This modeling of hysteretic fields is now generalized to include the anisotropic magnetization property caused by the lamination of iron sheets, and improved with respect to the time discretization method.

INTRODUCTION

The success of the Saito equation in the modeling of hysteretic magnetic fields had spurred the lumped circuit model for nonlinear inductors exhibiting hysteresis loops [2]. Also, this Saito equation was extended to take into account the anisotropy caused by the lamination of iron sheets for calculating three-dimensional magnetic fields in a toroidal transformer [3].

Furthermore, it was reported that the Saito equation was closely related with the Preisach type model and the fluctuation after effect proposed by Néel [4,5].

In this paper, the improved modeling of hysteretic and anisotropic fields proposed in [3] is applied to a toroidal reactor. Consequently, it is confirmed that our modeling of hysteretic and anisotropic magnetic fields gives excellent results compared with those of [1].

MODELING OF HYSTERETIC AND ANISOTROPIC FIELDS

A specific hysteresis model is given by

$$H = (1/\mu)B + (1/s)\partial B/\partial t, \qquad (1)$$

where H,B,μ,s and t denote the field intensity, flux density, permeability, hysteresis coefficient, and time respectively. The permeability μ and hysteresis coefficient s are nonlinear functions of B and ∂B/∂t as shown in Fig. 1. For further details of Formula (1), you may refer to [1-5].

In order to suppress the eddy currents flowing through the iron core, electromagnetic devices are always constructed of laminations, using insulated iron sheets. This makes the magnetization characteristics of the iron core anisotropic in direction.

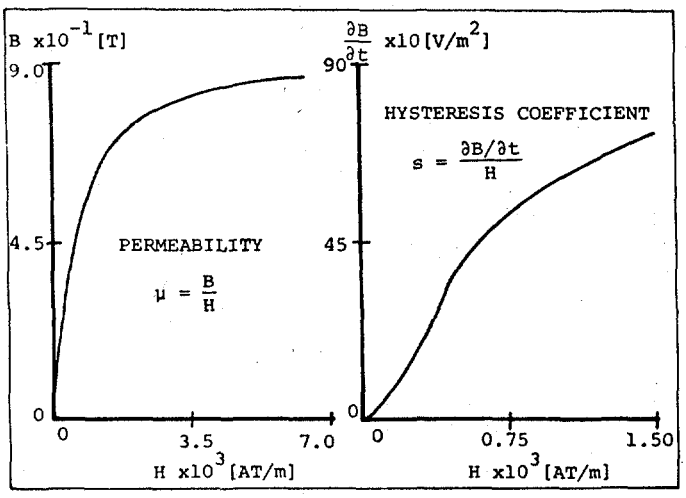

Fig. 1. Magnetization curves for μ and s.

Y. Saito, s. Hayano and T. yamamura are with College of Engineering, Hosei University, Kajinocho Koganei, Tokyo 184, Japan. H. Saotome is with Fuji Electric Co. Ltd., 1 Fujicho Hino, Tokyo 191, Japan.

For an example, let's consider the magnetization property of the iron core shown in Fig. 2; there it is obvious that the permeability μ and hysteresis coefficient s of this iron core may take different values with respect to direction. Generally, the space occupied by the insulation materials in the iron core is very small, and may be regarded as an air gap. Furthermore, the permeability μ of air is very small compared with that of iron, and the hysteresis coefficient s takes an infinitely large value. Thereby it is a reasonable assumption that all of the flux in the direction of the x-axis in Fig. 2 will flow through the path containing iron. This assumption yields the permeability μ_x and hysteresis coefficient s_x as

$$\begin{vmatrix} \mu_x \\ s_x \end{vmatrix} = \begin{vmatrix} \gamma & 0 \\ 0 & \gamma \end{vmatrix} \times \begin{vmatrix} \mu \\ s \end{vmatrix}, \qquad (2)$$

where γ is the space factor of iron viz., γ=[VOLUME OF IRON]/[TOTAL VOLUME OF IRON CORE].

On the contrary, all of the flux in the direction of the y-axis in Fig. 2 must flow through the path containing iron as well as air. This means that the permeability μ_y and hysteresis coefficient s_y in Fig. 2 are given by

$$\begin{vmatrix} \mu_y \\ s_y \end{vmatrix} = \begin{vmatrix} 1/[\gamma+\{\mu/\mu_0(1-\gamma)\}] & 0 \\ 0 & 1/\gamma \end{vmatrix} \times \begin{vmatrix} \mu \\ s \end{vmatrix}, \qquad (3)$$

where μ_0 is the permeability of air. (2) and (3) have been derived for a simple rectangular prism element. However, the results are still valid for the other shapes of element.

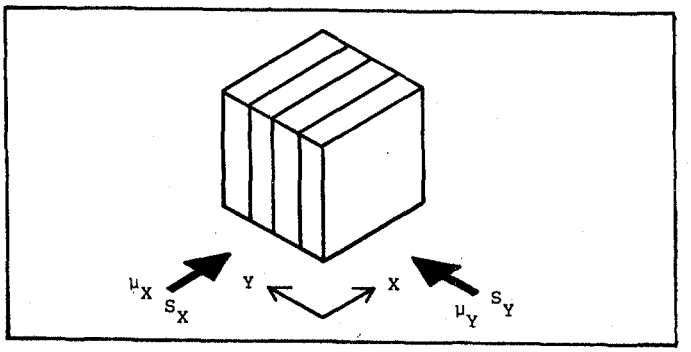

Fig. 2. An example of laminated core.

METHOD OF MAGNETIC CIRCUITS

As shown in Fig. 3(a), the toroidal reactor consists of conducting wires around an iron core. Generally, the magnetic flux which passes through the path parallel to the current-carrying coil can be neglected. Thereby, it is preferable to consider the solid element shown in Fig. 3(b). This solid element can be represented by the coordinates consisting of radial and tangential directions. The reactor shown in Fig. 3(a) is subdivided into M solid elements, taking into account the region containing air as well as coils. Thereby, the magnetic field calculation of the reactor may be reduced to evaluating the M loop fluxes.

However, when we compare the schematic diagram of the reactor in Fig. 3(a) with its magnetic circuits in Fig. 3(c), then it is found that the loop flux ϕ_{M+1} shown in dotted line in Fig. 3(c) must be taken into

0018-9464/84/0900-1965$01.00©1984 IEEE

account in the calculation to satisfy the condition of minimum number of network equations.

In order to derive the two-dimensional relations, let us consider the mesh points on the x-y plane, then it is assumed that the current densities are not uniformly distributed on the x-y plane but concentrated on the conductors with infinitesimally small cross sectional area located at each of their mesh points. Also, it is assumed that the region which encloses each of the mesh points may have a distinct permeability and hysteresis coefficient. Furthermore, the field intensity H and flux density B may take different values according to the positions, but it is possible to assume that each of the fluxes which flows through the paths between the mesh points takes a constant value.

With these assumptions, the magnetic fields in the x-y plane may be calculated for a modified form in the regions shown in Fig. 4(a). Applying (1) to the nodes a and b in Fig. 4(a) yields

$$\widehat{ab}\int Hdl = f_{\widehat{ab}} = \widehat{ab}\int[(1/\mu)B + (1/s)\partial B/\partial t]dl$$

$$= R_A\phi_A + S_A(\partial\phi_A/\partial t) = R_B\phi_B + S_B(\partial\phi_B/\partial t), \qquad (4)$$

where dl denotes an infinitesimally small distance along with the contour $\widehat{ab}$; R_A, R_B are the magnetic resistances; S_A, S_B are the hysteresis parameters; and ϕ_A, ϕ_B are the fluxes shown in Fig. 4(b). The details of these parameters are described in [1,3,6].

Denoting Δt as the stepwidth in time, (4) is discretized in time by

$$f_{\widehat{ab}}(t+\alpha\Delta t) = z_A^p(t+\alpha\Delta t)\phi_A(t+\Delta t) - z_A^n(t+\alpha\Delta t)\phi_A(t)$$

$$= z_B^p(t+\alpha\Delta t)\phi_B(t+\Delta t) - z_B^n(t+\alpha\Delta t)\phi_B(t), \qquad (5)$$

where

$$0 \le \alpha \le 1,$$

$$z_A^p(t+\alpha\Delta t) = (1/\Delta t)[S_A(t+\alpha\Delta t) + \alpha\Delta t R_A(t+\alpha\Delta t)],$$

$$z_A^n(t+\alpha\Delta t) = (1/\Delta t)[S_A(t+\alpha\Delta t) - \alpha\Delta t R_A(t+\alpha\Delta t)],$$

$$z_B^p(t+\alpha\Delta t) = (1/\Delta t)[S_B(t+\alpha\Delta t) + \alpha\Delta t R_B(t+\alpha\Delta t)], \qquad (6)$$

$$z_B^n(t+\alpha\Delta t) = (1/\Delta t)[S_B(t+\alpha\Delta t) - \alpha\Delta t R_B(t+\alpha\Delta t)].$$

In order to represent (5) in terms of loop fluxes in Fig. 4(a), it is assumed that the terms related to the time $t+\Delta t$ and t respectively correspond to each other in (5). This assumption modifies (5) to

$$f_{\widehat{ab}}(t+\alpha\Delta t) = z_{12}^p(t+\alpha\Delta t)[\phi_1(t+\Delta t) - \phi_2(t+\Delta t)]$$

$$- z_{12}^n(t+\alpha\Delta t)[\phi_1(t) - \phi_2(t)], \qquad (7)$$

where

$$z_{12}^p(t+\alpha\Delta t) = \frac{z_A^p(t+\alpha\Delta t)z_B^p(t+\alpha\Delta t)}{z_A^p(t+\alpha\Delta t)+z_B^p(t+\alpha\Delta t)},$$

$$z_{12}^n(t+\alpha\Delta t) = \frac{z_A^n(t+\alpha\Delta t)z_B^n(t+\alpha\Delta t)}{z_A^n(t+\alpha\Delta t)+z_B^n(t+\alpha\Delta t)}. \qquad (8)$$

The other magnetic circuit equations between the nodes are derived in much the same way as (7). Since the total magnetomotive force along with the contour $\widehat{abcda}$ must be equivalent to i_1 in Fig. 4(a), this gives

$$f_{\widehat{abcda}} = i_1 = (1/r_1)[e_1 - (\partial\phi_1/\partial t)], \qquad (9)$$

where e_1 is the externally impressed voltage. The electric resistance r_1 is defined in the direction of the z-axis in Fig. 4(a). The time discretized form of (9) is given by

$$f_{\widehat{abcda}}(t+\alpha\Delta t) = (1/r_1)[e_1(t+\alpha\Delta t)$$

$$- (1/\Delta t)\{\phi_1(t+\Delta t) - \phi_1(t)\}]. \qquad (10)$$

By combining (10) with the magnetic circuit equations enclosing the mesh point 1 in Fig. 4(a), it is possible to obtain the complete magnetic circuit equation related to the mesh point 1 in Fig. 4(a). The system of two-dimensional magnetic circuit equations is best expressed in matrix notation involoving the voltage vector $E[t+\alpha\Delta t]$, initial flux vector $\Phi[t]$, flux vector $\Phi[t+\Delta t]$, electric conductance matrix G, winding matrix W (see [1]), initial magnetic impedance matrix $Z^n[t+\alpha\Delta t]$ (see [3]) and magnetic impedance matrix $Z^p[t+\alpha\Delta t]$, viz.,

$$WGE[t+\alpha\Delta t] + \{WGW + Z^n[t+\alpha\Delta t]\}\Phi[t]$$

$$= \{WGW + Z^p[t+\alpha\Delta t]\}\Phi[t+\alpha\Delta t]\}\Phi[t+\Delta t]. \qquad (11)$$

As shown in Fig. 3(a), the loop flux ϕ_{M+1} is physically flowing in a tangential direction at the center of the iron core, so that this flux must be linked with all of the other circuits. This means that the loop flux ϕ_{M+1} is three-dimensionally introduced into the calculation by

$$\Phi[t] = C^T\phi_c[t], \quad \Phi[t+\Delta t] = C^T\phi_c[t+\Delta t], \qquad (12)$$

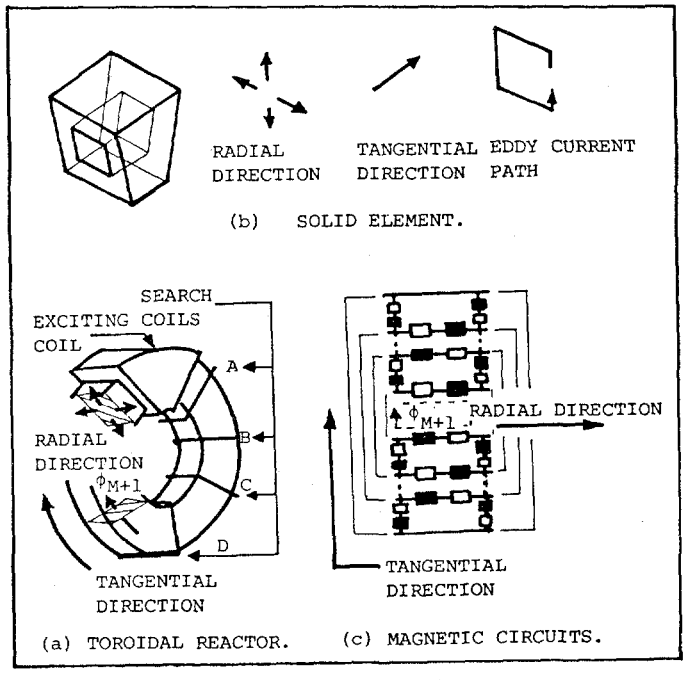

Fig. 3. Modeling of the toroidal reactor.

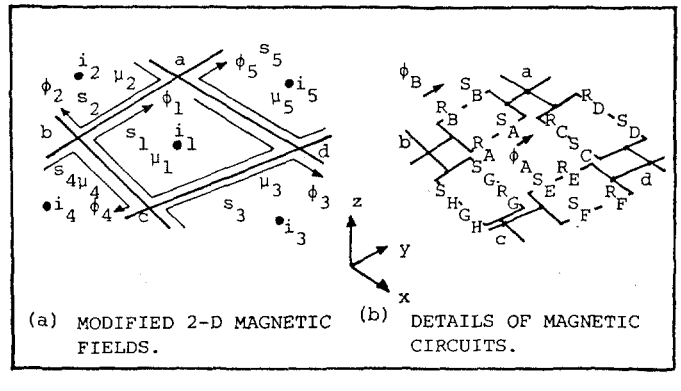

Fig. 4. Two-dimensional magnetic fields.

where subscript c refers to the three-dimensional quantities; superscript T denotes the transpose of a matrix; and C^T is the flux connection matrix which is a rectangular matrix with M rows and M+1 columns:

$$C^T = \begin{vmatrix} 1 & 0 & 0 & . & -1 \\ 0 & 1 & 0 & . & -1 \\ . & . & . & . & . \\ 0 & 0 & 0 & . & -1 \end{vmatrix} . \qquad (13)$$

By means of the flux connection matrix, the system of three-dimensional magnetic circuit equations is derived as

$$E_c[t+\alpha\Delta t] + \{G_c + Z_c^n[t+\alpha\Delta t]\}\Phi_c[t] = \{G_c + Z_c^p[t+\alpha\Delta t]\}\Phi_c[t+\alpha\Delta t], \qquad (14)$$

where

$$\left.\begin{aligned} E_c[t+\alpha\Delta t] &= CWE[t+\alpha\Delta t], \quad G_c = CWGWC^T, \\ Z_c^p[t+\alpha\Delta t] &= CZ^p[t+\alpha\Delta t]C^T, \\ Z_c^n[t+\alpha\Delta t] &= CZ^n[t+\alpha\Delta t]C^T. \end{aligned}\right| \qquad (15)$$

NUMERICAL SOLUTIONS AND CONCLUDING REMARKS

The parameter α and stepwidth Δt in (14) were respectively selected as $\alpha=0.5$ and $\Delta t=0.25$(msec) by the numerical tests when the convergence and accuracy of the solution were taken into account. The solution vector $\Phi_c[t+\Delta t]$ in (14) was calculated by iteration, using a relaxation parameter [1]. For comparison, the various constants used in the calculation were set to the same values as those of [1]. Fig. 1 shows the magnetization curves used in the calculation.

As a result, the method of the present paper yielded excellent results and remarkably improved the solutions obtained in [1]. Fig. 5 shows the representative results together with those of experiments.

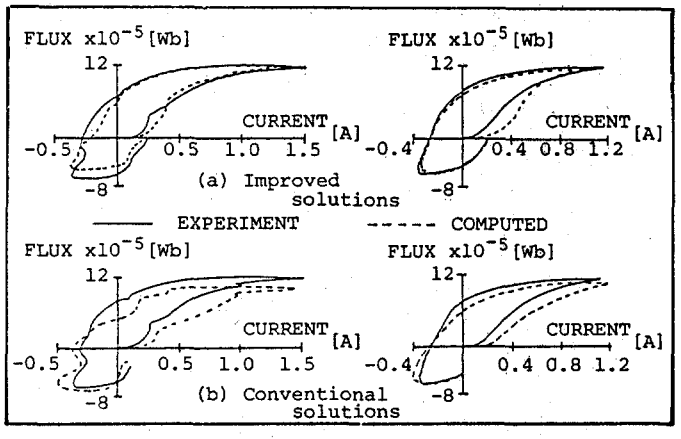

Fig.5 Examples of numerical solutions.

REFERENCES

[1] Y. Saito, "Three-dimensional Analysis of Magnetodynamic Fields in Electromagnetic Devices taken into account the Dynamic Hysteresis Loops," IEEE Trans. Magnetics, Vol. MAG-18, No. 2, March 1982, pp. 546-551.

[2] Y. Saito, H. Saotome, S. Hayano and T. Yamamura, "Modeling of Nonlinear Inductor exhibiting Hysteresis Loops and its Application to the Single Phase Parallel Inverters," IEEE Trans. Magnetics, Vol. MAG-19, No. 5, September 1983, pp. 2189-2191.

[3] Y. Saito, H. Saotome, S. Hayano and T. Yamamura, "Modeling of Hysteretic and Anisotropic Magnetic Fields," IEEE Trans. Magnetics, to be published in November issue in 1983.

[4] N. Tsuya, Y. Saito and S. Hayano, "A Study of Magnetic Hysteresis," Papers of Technical Meeting on Magnetics, IEE Japan, OKINAWA January 26, 1984.

[5] Y. Saito, S. Hayano, T. Yamamura and N. Tsuya, "A Representation of Magnetic Hysteresis," to be presented INTERMAG'84 at HAMBURG, April 10-13,1984.

[6] Y. Saito, "Three-dimensional Analysis of Nonlinear Magnetodynamic Fields in a Saturable Reactor," Comp. Meths. Appl. Mech. Eng., Vol. 22, No. 3, June 1980, pp. 289-308.